THE JOURNAL OF PHYSICAL CHEMISTRY LETTERS
A JOURNAL OF THE AMERICAN CHEMICAL SOCIETY

pubs.acs.org/JPCL

Letter

Allosteric Cross-Talk among Spike's Receptor-Binding Domain Mutations of the SARS-CoV-2 South African Variant Triggers an Effective Hijacking of Human Cell Receptor

Angelo Spinello, Andrea Saltalamacchia, Jure Borišek, and Alessandra Magistrato*

Cite This: J. Phys. Chem. Lett. 2021, 12, 5987−5993

Read Online

ACCESS | Metrics & More | Article Recommendations | Supporting Information

ABSTRACT: The rapid and relentless emergence of novel highly transmissible SARS-CoV-2 variants, possibly decreasing vaccine efficacy, currently represents a formidable medical and societal challenge. These variants frequently hold mutations on the Spike protein's receptor-binding domain (RBD), which, binding to the angiotensin-converting enzyme 2 (ACE2) receptor, mediates viral entry into host cells. Here, all-atom molecular dynamics simulations and dynamical network theory of the wild-type and mutant RBD/ACE2 adducts disclose that while the N501Y mutation (UK variant) enhances the Spike's binding affinity toward ACE2, the concomitant N501Y, E484K, and K417N mutations (South African variant) aptly adapt to increase SARS-CoV-2 propagation via a two-pronged strategy: (i) effectively grasping ACE2 through an allosteric signaling between pivotal RBD structural elements and (ii) impairing the binding of antibodies elicited by infected or vaccinated patients. This information unlocks the molecular terms and evolutionary strategies underlying the increased virulence of emerging SARS-CoV-2 variants, setting the basis for developing the next-generation anti-COVID-19 therapeutics.

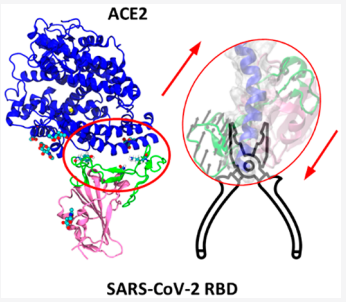

The severe acute respiratory syndrome coronavirus 2 (SARS-CoV-2), the etiological agent of coronavirus disease 19 (COVID-19), has infected as of April 30, 2021 about 150 million patients, causing over 3 million deaths worldwide. Owing to an unprecedentedly intense and relentless scientific effort, a variety of vaccines and monoclonal antibodies are becoming available for COVID-19 prophylaxis and therapeutic treatment.[1−3]

Similar to other β-coronaviruses (β-CoVs), the receptor-binding domain (RBD) of the homotrimeric viral spike (S) protein of SARS-CoV-2 mediates the molecular recognition and the binding to the human cellular receptor, angiotensin-converting enzyme 2 (ACE2),[4,5] thus triggering SARS-CoV-2 entry into host cells. As such, the S-protein has been the object of burgeoning research interest, becoming the prominent target for antibody development. This prompted an exhaustive experimental[6−8] and computational[9−18] assessment of the molecular interactions between the S-protein and ACE2.

The worldwide continuous and uncontrolled transmission of SARS-CoV-2 set the condition for its rapid evolution into more infectious variants. As an example, one of the first S-protein mutations, D614G, characterized by an enhanced transmissibility, has rapidly become dominant.[19] As well, other alarming strains have emerged in United Kingdom (lineage B.1.1.7),[20] South Africa (lineage B.1.351),[21] and Brazil (lineage P.1),[22] hereafter termed the UK, SA, and BR variants, respectively. Ultimately, a new dire Indian variant (lineage B.1.617) came to the fore. These lineages are the object of rising concerns owing to their increased transmissibility and/or their potential ability to elude infection- or vaccine-induced immunity.

As concerns the most prominent nonsynonymous mutations placed in the S-protein's RBD, most SARS-CoV-2 variants share the N501Y substitution (Figure 1), most likely implicated into an enhanced binding affinity toward ACE2,[23−25] although preliminary reports indicate that this variant retains vaccine efficacy.[26] In addition to N501Y, the SA variant also exhibits the E484K and K417N RBD mutations. E484, the most frequently mutated residue in COVID-19 patients, becomes E484K in the SA and BR and E484Q in the Indian strains. As well, mutation of K417, either to N or a T, is shared by the SA and BR variants, respectively. These mutations have been linked to viral escape from mAbs developed by vaccinated or infected patients.[2,27,28]

Aiming to dissect at the atomic level the role of RBD mutations on the recognition of ACE2, we performed cumulative 15 μs all-atom molecular dynamics (MD) simulations of S-protein RBD/ACE2 complexes considering the RBD's mutations present in the SA variant either concurrently or singularly.

Received: May 1, 2021
Accepted: June 21, 2021
Published: June 23, 2021

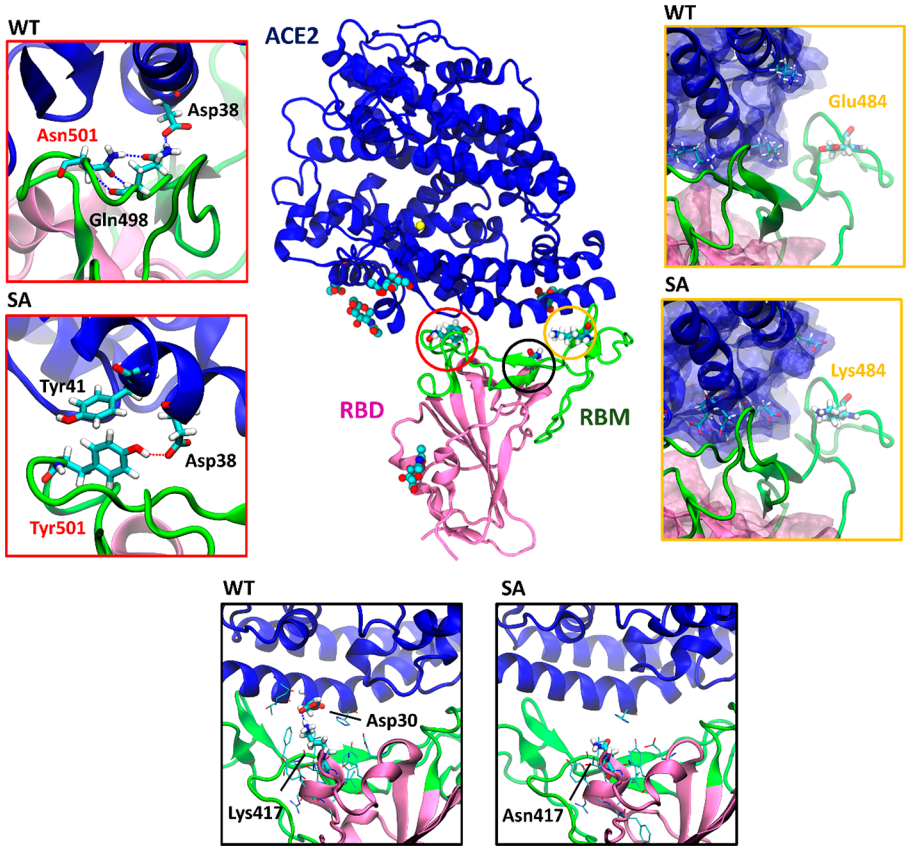

Figure 1. Representative structures of the complex between the South African (SA) SARS-CoV-2 variant of the receptor-binding domain (RBD, pink, with the receptor-binding motif (RBM) highlighted in green) and the angiotensin-converting enzyme 2 (ACE2, blue) as extracted from molecular dynamics trajectories. The three N501Y, E484K, and K417N mutations sites are circled in red, yellow, and black, respectively. The insets show a comparison of the key intermolecular interactions at the mutation sites in the wild-type (WT) and SA RBD/ACE2 complexes with residues depicted in licorice and hydrogen bonds displayed as dashed lines.

Namely, we first built the adduct between ACE2 and RBD carrying the N501Y, E484K, and K417N substitutions of the SA lineage (hereafter termed ^{SA}RBD/ACE2). Next, to inspect the role of each mutation, we built three distinct RBD/ACE2 models carrying N501Y (^{N501Y}RBD/ACE2 or ^{UK}RBD/ACE2), E484K (^{E484K}RBD/ACE2), and K417N (^{K417N}RBD/ACE2), ultimately comparing them with the WT RBD/ACE2 adduct (hereafter named RBD/ACE2). As a result, all the systems retain stable interactions at the RBD/ACE2 interface when performing 2.5 μs MD simulations for each system (Figure S1). Most of the RBD residues binding to ACE2 lie within the receptor-binding motif (RBM), which is composed by two small β-strands and 4 flexible loops. In a previous study, we pinpointed the rigidity of RBD Loop3 (L3, composed by Thr470-Pro491) as the main factor underlying the larger binding affinity of SARS-CoV-2 toward ACE2,[9] with respect to the closely related SARS-CoV. In the current set of MD simulations all the investigated systems evidence a similar RBMs flexibility, with small differences being restricted to Loop1 and 4 (L1/4, Figure S2), where N501Y is placed (Figure 1).

Although not engaging direct interactions with ACE2, in the WT adduct N501@RBD intramolecularly H-bonds to Gln498, mediating the formation of a persistent H-bond network between the latter residue and Asp38@ACE2 (Figure 1), thus being the most dynamically correlated residue of the whole RBM (Figure S3).[9,29] Nonetheless, in the ^{SA}RBD/ACE2 and ^{N501Y}RBD/ACE2 complexes, the Y501 further reinforces its prominent role in hijacking ACE2 by establishing π-stacking interactions with Tyr41@ACE2 (Figures 1 and S4 and Table S1) and directly H-bonding to Asp38@ACE2, consistent with the ^{N501Y}S-protein/ACE2 cryo-EM structure.[30] A similar H-bond pattern is also observed in μs-long MD simulations of RBD/ACE2 performed with a different force field (Table S2).[18]

Although the total binding free energies (ΔG_b) of the distinct RBD/ACE2 adducts, calculated with the molecular mechanics/generalized born surface area (MM-GBSA) method,[31] do not enable one to discriminate the subtle differences between WT and mutant RBD/ACE2 adducts (Table S3), a dissection of the per-residue amino acids ΔG_b contributions showed an increase, related to the N501Y substitution, with respect to the WT by 3.8 $\pm$ 2.0 and 4.4 $\pm$ 2.0 kcal/mol in ^{SA}RBD/ACE2 and ^{N501Y}RBD/ACE2, respectively (Figure S4), in agreement with recently reported theoretical[18] and experimental evidence.[24]

As such, N501Y, present in the highly infective UK and SA variants, possibly increases the RBD binding affinity for ACE2.[24,25] This comes along with a more effective grasping and bending of the ACE2's α1-helix in both ^{N501Y}RBD/ACE2 and ^{SA}RBD/ACE2 models as compared to RBD/ACE2 (Figure 2).

We also inspected the role of the E484K mutation common to the SA and BR variants for which no significant and reliable variation of the ΔG_b could be calculated (Figures S4 and S5) in ^{SA}RBD/ACE2 and ^{E484K}RBD/ACE2, respectively. Remark-

https://doi.org/10.1021/acs.jpclett.1c01415
J. Phys. Chem. Lett. 2021, 12, 5987−5993

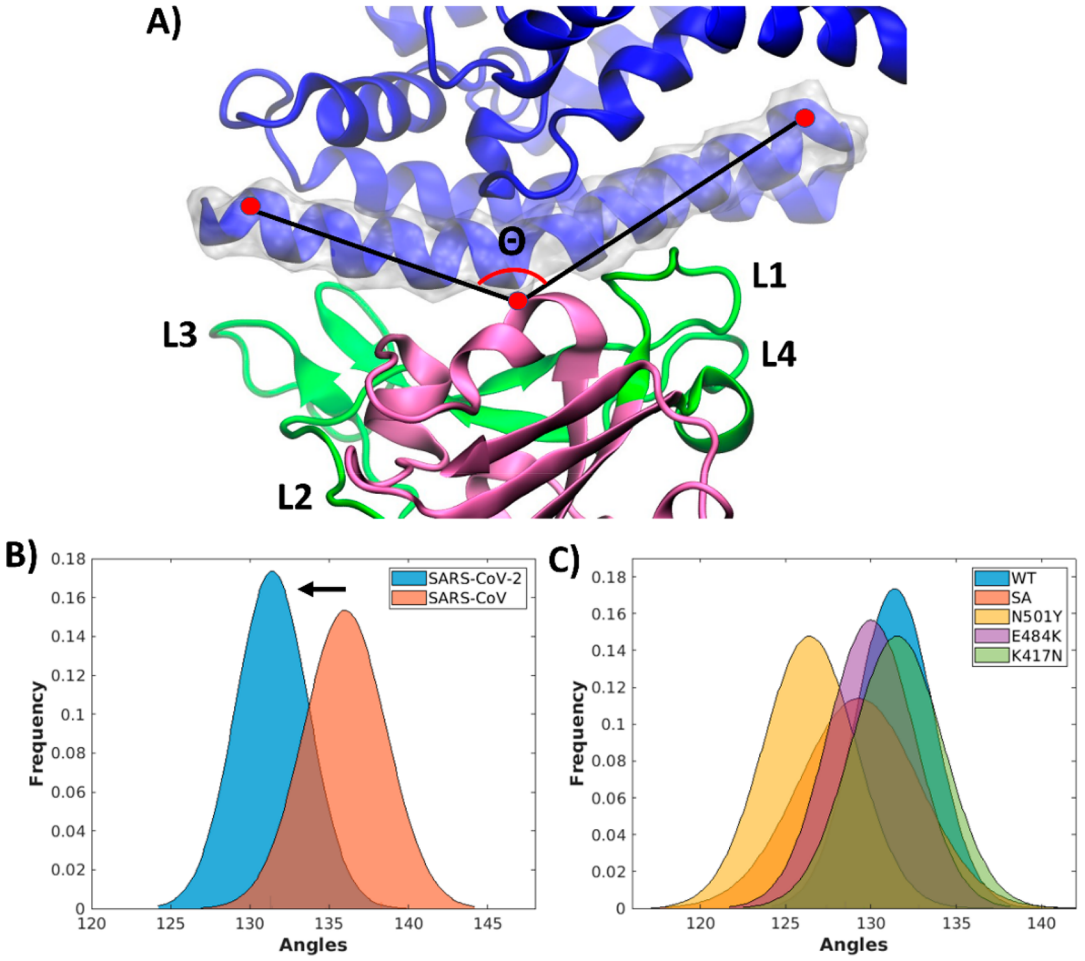

Figure 2. (A) Bending angle (Θ) of the angiotensin-converting enzyme 2 (ACE2)'s α1-helix defined by the Cα atoms of Phe22, Asn53, and Trp69. The receptor-binding domain (RBD), motif (RBM), and ACE2 are displayed in pink, green, and blue new-cartoons, respectively. The α1-helix@ACE2 is highlighted in silver transparent surface. (B) Distribution of Θ angle (deg) for SARS-CoV-2 and SARS-CoV RBD/ACE2[9] and (C) for SARS-CoV-2 RBD/ACE2, ^{SA}RBD/ACE2, ^{N501Y}RBD/ACE2, ^{E484K}RBD/ACE2, and ^{K417N}RBD/ACE2 models.

ably, K484 only modestly increases α1@ACE2 bending, as compared to the WT model (Figure 2C).

We finally assessed the role of K417,[21] whose salt-bridge with Asp30@ACE2, present in half of the RBD/ACE2 MD trajectory, is lost upon K417N mutation (Table S1). No significant variation of the ΔG_b could be observed for ^{K417N}RBD/ACE2 and ^{SA}RBD/ACE2 as compared to RBD/ACE2 (Figures S4 and S6),[24] and K417N does not increase the α1-helix@ACE2 bending (Figure 2). Hence, the way K417N contributes to enhance the ACE2 sequestration remains elusive.

Because of the strategic location of K417, halfway of L1/4 and L3 in the RBM, tweezing the α1-helix@ACE2, we computed the cross-correlation matrices based on the Pearson's correlation coefficient (CCs) and the per-residue sum of the cross-correlation coefficient (CCc) for the residues at the RBM/ACE2 interface (namely, we consider for each RBM residue the sum of the CCs calculated with respect to all residues of the ACE2 surface, Figure S3).[32,33] As a result, in ^{SA}RBD/ACE2 and ^{K417}RBD/ACE2, the residues of the RBM exhibit the largest per-residue CCc's. The CCs increase of ^{SA}RBD/ACE2 is more marked at the L1/4 and L3 regions.

Aiming to assess whether the mutations could interfere with the RBD's slow motions, we performed principal component (PC) analysis of WT and mutant RBD models to gather their most relevant movements (essential dynamics). As a result, PC1 and 2 of WT or all mutant RBD systems reveal the opening/closing motions of L1/4 and L3 regions, which are implicated in grasping α1-helix@ACE2 (Figure S7). Because an allosteric communication among SARS-CoV-2 mutations has been recently speculated,[34−36] we then applied dynamical network theory analysis (NWA) to decrypt the information-exchange pathways underlying the observed RBD functional dynamics and to decode whether RBD mutants can enhance the allosteric cross-talk between critical RBD's structural elements.[32,37,38] In NWA, the protein is represented as a correlation-based weighted network. The nodes (the residues' center of mass) are connected by edges whose numerical value (weight) indicates the correlation-strength between residue pairs (i.e., small/large weights reflect highly/poorly correlated and anticorrelated motions). By computing cross-correlations between residues along an MD trajectory, NWA finds the optimal and suboptimal signaling paths between two user-selected source (484@L3) and sink (501@L4) residues. The outcoming path lengths are thus inversely proportional to the signaling strength and to the amount of correlation existing among their tracing nodes.[37]

By performing NWA on the RBD alone we observed several cross-communication paths crossing the RBM, which in RBD/ACE2 minorly involve even K417 (Figure 3B,D). Remarkably,

https://doi.org/10.1021/acs.jpclett.1c01415
J. Phys. Chem. Lett. 2021, 12, 5987−5993

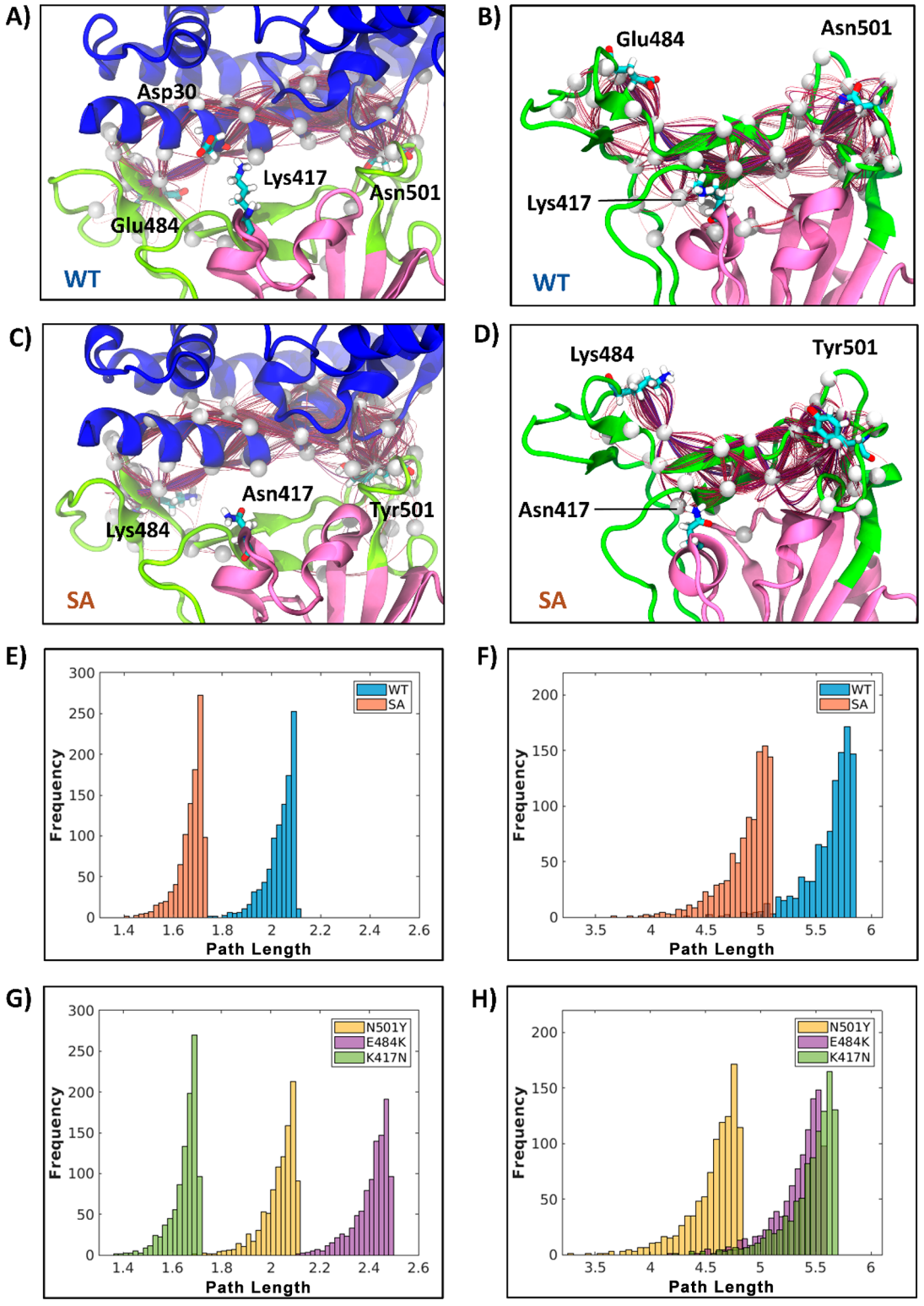

Figure 3. Optimal and suboptimal signaling paths (red lines, with nodes depicted as white spheres) connecting the receptor-binding domain (RBD) residues 484 and 501, for (A) wild type (WT) RBD/angiotensin-converting enzyme 2 (ACE2), (B) WT RBD, (C) South African ^{SA}RBD/ACE2, and (D) ^{SA}RBD. Distribution of signaling path lengths for (E) WT RBD/ACE2 and ^{SA}RBD/ACE2 adducts, (F) WT and SA isolated RBDs, (G) all investigated single mutants in the RBD/ACE2 adducts, and (H) all the isolated mutants in the RBDs.

in $^{N501Y(UK)}$RBD and ^{SA}RBD these paths are shorter (the residues are more correlated, Figure 3F,H), suggesting a stronger signaling between the two RBM extremities, which may result in a more effective opening/closing of the L1/4 and L3.

In all RBD/ACE2 models this allosteric signaling within RBM occurs along the α1-helix@ACE2 (Figure 3A,C), and the path-length distribution of both ^{SA}RBD/ACE2 and ^{K417N}RBD/ACE2 (Figure 3E,G) is shifted toward lower values. This suggests that the motions of RBM's residues are more tightly

https://doi.org/10.1021/acs.jpclett.1c01415
J. Phys. Chem. Lett. 2021, 12, 5987−5993

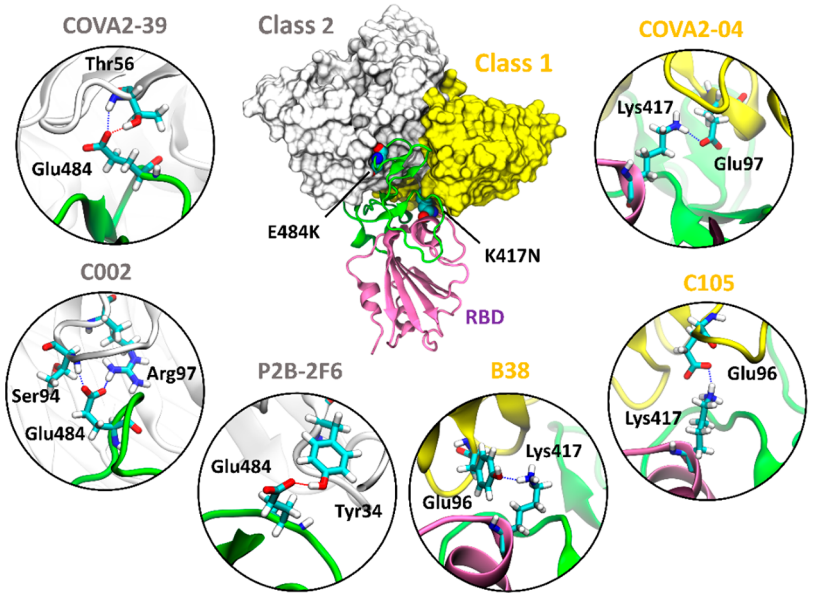

Figure 4. Binding mode of class 1 and class 2 (yellow and gray surfaces) monoclonal antibodies (mAbs) isolated from patients to the Spike's receptor-binding domain (RBD), showing the use of different epitopes. The receptor-binding motif (RBM) and RBD are shown as green and pink new-cartoons, respectively. Insets disclose the key intermolecular interactions established between (from left to right) the mAbs COVA2-39,[40] C002,[41] P2B-2F6,[42] B38,[43] C105,[44] and COVA2-04.[40]

correlated and trigger a more effective ACE2 hijacking. The similar distribution observed for ^{SA}RBD/ACE2 and ^{K417N}RBD/ACE2 indicates that K417N is primarily liable for the enhanced cross-talk between critical RBD recognition loops (Figure 3E,G). A test of the dependence of the calculated paths from the source/sink selection (Figure S8) has been performed showing that the general trend observed in Figure 3E,F is maintained. However, we cannot exclude that considering a larger model of the S protein or an additional mutation present far from the RBD may perturb the observed signaling routes.[39]

To identify the residues critically involved in the signaling pathways we computed the node degeneracy (i.e., the number of times a node is present in the calculated paths). In the presence of the RBD mutations a significant variation in degeneracy is observed for those residues engaging H-bond or hydrophobic interactions at the RBD/ACE2 interface, among which are Asp38@ACE2, Asp355@ACE2, and Thr500@RBD (Figure S9 and Table S4). To further dissect the source of the increased cross-talk in the mutant RBD/ACE2 complexes we inspected whether RBD mutations alter the intra-RBD H-bonds network at the RBD/ACE2 interface. Interestingly, the main differences among the investigated systems are localized on L3−4, near the mutation sites (Table S5). In particular, a decrease of the intramolecular H-bond persistence of Asn487, which strongly H-bonds to ACE2 (Table S1), results in a higher node-degeneracy (i.e., a relevant role along the signaling route) (Table S4).

Complementarily, structural X-ray and Cryo-EM studies elucidated that K417 and E484 RBD residues establish H-bonds with distinct mAbs isolated from COVID-19 patients' sera. Hence, K417N and E484K substitutions alter the electrostatic complementarity between the RBD and class 1 and 2 mAbs, respectively (Figure 4 and Table S6),[40−45] impairing mAbs binding and contributing to viral escape from vaccine/disease-induced immunity.[2,41]

In summary, aiming to dissect the molecular basis for the higher infectivity and transmissibility of emerging SARS-CoV-2 variants, we have assessed the impact of the SA set of RBD mutations, considering them either concurrently or singularly. As a result, we disclose that while N501Y (hallmark of the UK variant) enhances the binding affinity toward ACE2 and increases the α1-helix@ACE2 bending, the SA strain exploits a two-pronged strategy to more effectively infect the host cells by (i) increasing the allosteric signaling among the pivotal RBM loops, which acting as a tweezer more effectively grasp/bend α1-helix@ACE2 and (ii) hindering the interactions with class 1 and 2 mAbs (K417N and E484K, respectively) extracted from COVID-19 patients' sera (Figure 4 and Table S6). Stunningly, the main actor in modulating the allosteric cross-talk among the RBD mutants appears to be K417N, whose role has remained so far elusive. In this scenario, it is tempting to argue that the BR variant, differing from the SA one only by the K417T@RBD substitution, may exploit the same strategy to foster viral propagation. Our outcomes contribute to decrypting at the atomic level the evolutionary strategies underlying the increased SARS-CoV-2 infectivity and spreading of emerging variants, setting a conceptual basis to devise next-generation therapeutic strategies against current and future viral strains.

■ ASSOCIATED CONTENT

Supporting Information

The Supporting Information is available free of charge at https://pubs.acs.org/doi/10.1021/acs.jpclett.1c01415.

Computational Details, Figures S1−S9, and Tables S1−S6 (PDF)

https://doi.org/10.1021/acs.jpclett.1c01415
J. Phys. Chem. Lett. 2021, 12, 5987−5993

AUTHOR INFORMATION

Corresponding Author

Alessandra Magistrato − *CNR-IOM c/o SISSA, 34136 Trieste, Italy*; orcid.org/0000-0002-2003-1985; Email: alessandra.magistrato@sissa.it

Authors

Angelo Spinello − *CNR-IOM c/o SISSA, 34136 Trieste, Italy*; orcid.org/0000-0002-8387-8956

Andrea Saltalamacchia − *International School for Advanced Studies SISSA, 34136 Trieste, Italy*; orcid.org/0000-0003-1174-9271

Jure Borišek − *National Institute of Chemistry, 1000 Ljubljana, Slovenia*; orcid.org/0000-0003-3417-0940

Complete contact information is available at: https://pubs.acs.org/10.1021/acs.jpclett.1c01415

Notes

The authors declare no competing financial interest.

ACKNOWLEDGMENTS

A. Spinello was supported by a FIRC-AIRC "Mario e Valeria Rindi" fellowship for Italy. A. Magistrato acknowledges the financial support of the Italian Association for Cancer Research (AIRC) (IG Grant 24514) and of the project "Against bRain cancEr: finding personalized therapies with in Silico and in vitro strategies" (ARES) CUP:D93D19000020007 POR FESR 2014 2020-1.3.b-Friuli Venezia Giulia.

REFERENCES

(1) Hsieh, C. L.; Goldsmith, J. A.; Schaub, J. M.; DiVenere, A. M.; Kuo, H. C.; Javanmardi, K.; Le, K. C.; Wrapp, D.; Lee, A. G.; Liu, Y.; Chou, C. W.; Byrne, P. O.; Hjorth, C. K.; Johnson, N. V.; Ludes-Meyers, J.; Nguyen, A. W.; Park, J.; Wang, N.; Amengor, D.; Lavinder, J. J.; Ippolito, G. C.; Maynard, J. A.; Finkelstein, I. J.; McLellan, J. S. Structure-based design of prefusion-stabilized SARS-CoV-2 spikes. *Science* **2020**, *369* (6510), 1501−1505.

(2) Andreano, E.; Piccini, G.; Licastro, D.; Casalino, L.; Johnson, N. V.; Paciello, I.; Monego, S. D.; Pantano, E.; Manganaro, N.; Manenti, A.; Manna, R.; Casa, E.; Hyseni, I.; Benincasa, L.; Montomoli, E.; Amaro, R. E.; McLellan, J. S.; Rappuoli, R. SARS-CoV-2 escape in vitro from a highly neutralizing COVID-19 convalescent plasma. *bioRxiv* **2020**. DOI: 10.1101/2020.12.28.424451

(3) Serapian, S. A.; Marchetti, F.; Triveri, A.; Morra, G.; Meli, M.; Moroni, E.; Sautto, G. A.; Rasola, A.; Colombo, G. The Answer Lies in the Energy: How Simple Atomistic Molecular Dynamics Simulations May Hold the Key to Epitope Prediction on the Fully Glycosylated SARS-CoV-2 Spike Protein. *J. Phys. Chem. Lett.* **2020**, *11* (19), 8084−8093.

(4) Li, W.; Moore, M. J.; Vasilieva, N.; Sui, J.; Wong, S. K.; Berne, M. A.; Somasundaran, M.; Sullivan, J. L.; Luzuriaga, K.; Greenough, T. C.; Choe, H.; Farzan, M. Angiotensin-converting enzyme 2 is a functional receptor for the SARS coronavirus. *Nature* **2003**, *426* (6965), 450−4.

(5) Wang, Q.; Zhang, Y.; Wu, L.; Niu, S.; Song, C.; Zhang, Z.; Lu, G.; Qiao, C.; Hu, Y.; Yuen, K. Y.; Wang, Q.; Zhou, H.; Yan, J.; Qi, J. Structural and Functional Basis of SARS-CoV-2 Entry by Using Human ACE2. *Cell* **2020**, *181* (4), 894−904.

(6) Wrapp, D.; Wang, N.; Corbett, K. S.; Goldsmith, J. A.; Hsieh, C. L.; Abiona, O.; Graham, B. S.; McLellan, J. S. Cryo-EM structure of the 2019-nCoV spike in the prefusion conformation. *Science* **2020**, *367* (6483), 1260−1263.

(7) Shang, J.; Ye, G.; Shi, K.; Wan, Y.; Luo, C.; Aihara, H.; Geng, Q.; Auerbach, A.; Li, F. Structural basis of receptor recognition by SARS-CoV-2. *Nature* **2020**, *581*, 221.

(8) Tai, W.; He, L.; Zhang, X.; Pu, J.; Voronin, D.; Jiang, S.; Zhou, Y.; Du, L. Characterization of the receptor-binding domain (RBD) of 2019 novel coronavirus: implication for development of RBD protein as a viral attachment inhibitor and vaccine. *Cell. Mol. Immunol.* **2020**, *17*, 613.

(9) Spinello, A.; Saltalamacchia, A.; Magistrato, A. Is the Rigidity of SARS-CoV-2 Spike Receptor-Binding Motif the Hallmark for Its Enhanced Infectivity? Insights from All-Atom Simulations. *J. Phys. Chem. Lett.* **2020**, *11* (12), 4785−4790.

(10) Wang, Y.; Liu, M.; Gao, J. Enhanced receptor binding of SARS-CoV-2 through networks of hydrogen-bonding and hydrophobic interactions. *Proc. Natl. Acad. Sci. U. S. A.* **2020**, *117* (25), 13967−13974.

(11) Ali, A.; Vijayan, R. Dynamics of the ACE2-SARS-CoV-2/SARS-CoV spike protein interface reveal unique mechanisms. *Sci. Rep.* **2020**, *10* (1), 14214.

(12) Barros, E. P.; Casalino, L.; Gaieb, Z.; Dommer, A. C.; Wang, Y.; Fallon, L.; Raguette, L.; Belfon, K.; Simmerling, C.; Amaro, R. E. The flexibility of ACE2 in the context of SARS-CoV-2 infection. *Biophys. J.* **2021**, *120* (6), 1072−1084.

(13) Frances-Monerris, A.; Hognon, C.; Miclot, T.; Garcia-Iriepa, C.; Iriepa, I.; Terenzi, A.; Grandemange, S.; Barone, G.; Marazzi, M.; Monari, A. Molecular Basis of SARS-CoV-2 Infection and Rational Design of Potential Antiviral Agents: Modeling and Simulation Approaches. *J. Proteome Res.* **2020**, *19* (11), 4291−4315.

(14) Dehury, B.; Raina, V.; Misra, N.; Suar, M. Effect of mutation on structure, function and dynamics of receptor binding domain of human SARS-CoV-2 with host cell receptor ACE2: a molecular dynamics simulations study. *J. Biomol. Struct. Dyn.* **2020**, 1−15.

(15) Laurini, E.; Marson, D.; Aulic, S.; Fermeglia, A.; Pricl, S. Computational Mutagenesis at the SARS-CoV-2 Spike Protein/Angiotensin-Converting Enzyme 2 Binding Interface: Comparison with Experimental Evidence. *ACS Nano* **2021**, *15* (4), 6929−6948.

(16) Jafary, F.; Jafari, S.; Ganjalikhany, M. R. In silico investigation of critical binding pattern in SARS-CoV-2 spike protein with angiotensin-converting enzyme 2. *Sci. Rep.* **2021**, *11* (1), 6927.

(17) Miotto, M.; Di Rienzo, L.; Gosti, G.; Bò, L.; Parisi, G.; Piacentini, R.; Boffi, A.; Ruocco, G.; Milanetti, E. Inferring the stabilization effects of SARS-CoV-2 variants on the binding with ACE2 receptor. *BioRxiv* **2021**. DOI: 10.1101/2021.04.18.440345

(18) Pavlova, A.; Zhang, Z.; Acharya, A.; Lynch, D. L.; Pang, Y. T.; Mou, Z.; Parks, J. M.; Chipot, C.; Gumbart, J. C. Machine Learning Reveals the Critical Interactions for SARS-CoV-2 Spike Protein Binding to ACE2. *J. Phys. Chem. Lett.* **2021**, *12*, 5494−5502.

(19) Korber, B.; Fischer, W. M.; Gnanakaran, S.; Yoon, H.; Theiler, J.; Abfalterer, W.; Hengartner, N.; Giorgi, E. E.; Bhattacharya, T.; Foley, B.; Hastie, K. M.; Parker, M. D.; Partridge, D. G.; Evans, C. M.; Freeman, T. M.; de Silva, T. I.; Sheffield, C.-G. G.; McDanal, C.; Perez, L. G.; Tang, H.; Moon-Walker, A.; Whelan, S. P.; LaBranche, C. C.; Saphire, E. O.; Montefiori, D. C.; et al. Tracking Changes in SARS-CoV-2 Spike: Evidence that D614G Increases Infectivity of the COVID-19 Virus. *Cell* **2020**, *182* (4), 812−827.

(20) Davies, N. G.; Abbott, S.; Barnard, R. C.; Jarvis, C. I.; Kucharski, A. J.; Munday, J. D.; Pearson, C. A. B.; Russell, T. W.; Tully, D. C.; Washburne, A. D.; Wenseleers, T.; Gimma, A.; Waites, W.; Wong, K. L. M.; van Zandvoort, K.; Silverman, J. D.; Group, C. C.-W.; Consortium, C.-G. U.; Diaz-Ordaz, K.; Keogh, R.; Eggo, R. M.; Funk, S.; Jit, M.; Atkins, K. E.; Edmunds, W. J. Estimated transmissibility and impact of SARS-CoV-2 lineage B.1.1.7 in England. *Science* **2021**, *372* (6538), eabg3055.

(21) Tegally, H.; Wilkinson, E.; Giovanetti, M.; Iranzadeh, A.; Fonseca, V.; Giandhari, J.; Doolabh, D.; Pillay, S.; San, W. J.; Msoni, N.; Mlisana, K.; von Gottberg, A.; Walaza, S.; Allam, M.; Ismail, A.; Mohale, T.; Glass, A. J.; Engelbrecht, S.; Van Zyl, G.; Preiser, W.; Petruccione, F.; Sigal, A.; Hardie, D.; Marais, G.; Hsiao, M.; Korsman, S.; Davies, M.; Tyers, L.; Mudau, I.; York, D.; Maslo, C.; Goedhals, D.; Abrahams, S.; Laguda-Akingba, O.; Alisoltani-Dehkordi, A.; Godzik, A.; Wibmer, C. K.; Sewell, B. T.; Lourenco, J.; Alcantara, L. C.; Pond, S. L. K.; Weaver, S.; Martin, D.; Lessells, R. J.; Bhiman, J.

N.; Williamson, C.; de Oliveira, T. Emergence and rapid spread of a new severe acute respiratory syndrome-related coronavirus 2 (SARS-CoV-2) lineage with multiple spike mutations in South Africa. *medRxiv* **2020**. DOI: 10.1101/2020.12.21.20248640

(22) He, D.; Fan, G.; Wang, X.; Li, Y.; Peng, Z. The new SARS-CoV-2 variant and reinfection in the resurgence of COVID-19 outbreaks in Manaus, Brazil. *medRxiv* **2021**. DOI: 10.1101/2021.03.25.21254281

(23) Gu, H.; Chen, Q.; Yang, G.; He, L.; Fan, H.; Deng, Y. Q.; Wang, Y.; Teng, Y.; Zhao, Z.; Cui, Y.; Li, Y.; Li, X. F.; Li, J.; Zhang, N. N.; Yang, X.; Chen, S.; Guo, Y.; Zhao, G.; Wang, X.; Luo, D. Y.; Wang, H.; Yang, X.; Li, Y.; Han, G.; He, Y.; Zhou, X.; Geng, S.; Sheng, X.; Jiang, S.; Sun, S.; Qin, C. F.; Zhou, Y. Adaptation of SARS-CoV-2 in BALB/c mice for testing vaccine efficacy. *Science* **2020**, *369* (6511), 1603−1607.

(24) Starr, T. N.; Greaney, A. J.; Hilton, S. K.; Ellis, D.; Crawford, K. H. D.; Dingens, A. S.; Navarro, M. J.; Bowen, J. E.; Tortorici, M. A.; Walls, A. C.; King, N. P.; Veesler, D.; Bloom, J. D. Deep Mutational Scanning of SARS-CoV-2 Receptor Binding Domain Reveals Constraints on Folding and ACE2 Binding. *Cell* **2020**, *182* (5), 1295−1310.

(25) Tian, F.; Tong, B.; Sun, L.; Shi, S.; Zheng, B.; Wang, Z.; Dong, X.; Zheng, P. Mutation N501Y in RBD of Spike Protein Strengthens the Interaction between COVID-19 and its Receptor ACE2. *BioRxiv* **2021**. DOI: 10.1101/2021.02.14.431117

(26) Xie, X.; Liu, Y.; Liu, J.; Zhang, X.; Zou, J.; Fontes-Garfias, C. R.; Xia, H.; Swanson, K. A.; Cutler, M.; Cooper, D.; Menachery, V. D.; Weaver, S. C.; Dormitzer, P. R.; Shi, P. Y. Neutralization of SARS-CoV-2 spike 69/70 deletion, E484K and N501Y variants by BNT162b2 vaccine-elicited sera. *Nat. Med.* **2021**, *27*, 620.

(27) Greaney, A. J.; Starr, T. N.; Gilchuk, P.; Zost, S. J.; Binshtein, E.; Loes, A. N.; Hilton, S. K.; Huddleston, J.; Eguia, R.; Crawford, K. H. D.; Dingens, A. S.; Nargi, R. S.; Sutton, R. E.; Suryadevara, N.; Rothlauf, P. W.; Liu, Z.; Whelan, S. P. J.; Carnahan, R. H.; Crowe, J. E., Jr.; Bloom, J. D. Complete Mapping of Mutations to the SARS-CoV-2 Spike Receptor-Binding Domain that Escape Antibody Recognition. *Cell Host Microbe* **2021**, *29* (1), 44−57.

(28) Weisblum, Y.; Schmidt, F.; Zhang, F.; DaSilva, J.; Poston, D.; Lorenzi, J. C.; Muecksch, F.; Rutkowska, M.; Hoffmann, H. H.; Michailidis, E.; Gaebler, C.; Agudelo, M.; Cho, A.; Wang, Z.; Gazumyan, A.; Cipolla, M.; Luchsinger, L.; Hillyer, C. D.; Caskey, M.; Robbiani, D. F.; Rice, C. M.; Nussenzweig, M. C.; Hatziioannou, T.; Bieniasz, P. D. Escape from neutralizing antibodies by SARS-CoV-2 spike protein variants. *eLife* **2020**, *9*. DOI: 10.7554/eLife.61312

(29) Pavlin, M.; Spinello, A.; Pennati, M.; Zaffaroni, N.; Gobbi, S.; Bisi, A.; Colombo, G.; Magistrato, A. A Computational Assay of Estrogen Receptor alpha Antagonists Reveals the Key Common Structural Traits of Drugs Effectively Fighting Refractory Breast Cancers. *Sci. Rep.* **2018**, *8* (1), 649.

(30) Zhu, X.; Mannar, D.; Srivastava, S. S.; Berezuk, A. M.; Demers, J.; Saville, J. W.; Leopold, K.; Li, W.; Dimitrov, D. S.; Tuttle, K. S.; Zhou, S.; Chittori, S.; Subramaniam, S. Cryo-EM Structures of the N501Y SARS-CoV-2 Spike Protein in Complex with ACE2 and Two Potent Neutralizing Antibodies. *BioRxiv* **2021**. DOI: 10.1101/2021.01.11.426269

(31) Kollman, P. A.; Massova, I.; Reyes, C.; Kuhn, B.; Huo, S.; Chong, L.; Lee, M.; Lee, T.; Duan, Y.; Wang, W.; Donini, O.; Cieplak, P.; Srinivasan, J.; Case, D. A.; Cheatham, T. E., 3rd. Calculating structures and free energies of complex molecules: combining molecular mechanics and continuum models. *Acc. Chem. Res.* **2000**, *33* (12), 889−97.

(32) Saltalamacchia, A.; Casalino, L.; Borisek, J.; Batista, V. S.; Rivalta, I.; Magistrato, A. Decrypting the Information Exchange Pathways across the Spliceosome Machinery. *J. Am. Chem. Soc.* **2020**, *142* (18), 8403−8411.

(33) Casalino, L.; Palermo, G.; Spinello, A.; Rothlisberger, U.; Magistrato, A. All-atom simulations disentangle the functional dynamics underlying gene maturation in the intron lariat spliceosome. *Proc. Natl. Acad. Sci. U. S. A.* **2018**, *115* (26), 6584−6589.

(34) Verkhivker, G. M.; Agajanian, S.; Oztas, D. Y.; Gupta, G. Comparative Perturbation-Based Modeling of the SARS-CoV-2 Spike Protein Binding with Host Receptor and Neutralizing Antibodies: Structurally Adaptable Allosteric Communication Hotspots Define Spike Sites Targeted by Global Circulating Mutations. *BioRxiv* **2021**. DOI: 10.1101/2021.02.21.432165

(35) Nelson, G.; Buzko, O.; Spilman, P.; Niazi, K.; Rabizadeh, S.; Soon-Shiong, P. Molecular dynamic simulation reveals E484K mutation enhances spike RBD-ACE2 affinity and the combination of E484K, K417N and N501Y mutations (501Y.V2 variant) induces conformational change greater than N501Y mutant alone, potentially resulting in an escape mutant. *BioRxiv* **2021**. DOI: 10.1101/2021.01.13.426558

(36) Ray, D.; Le, L.; Andricioaei, I. Distant Residues Modulate Conformational Opening in SARS-CoV-2 Spike Protein. *BioRxiv* **2021**. DOI: 10.1101/2020.12.07.415596

(37) Van Wart, A. T.; Durrant, J.; Votapka, L.; Amaro, R. E. Weighted Implementation of Suboptimal Paths (WISP): An Optimized Algorithm and Tool for Dynamical Network Analysis. *J. Chem. Theory Comput.* **2014**, *10* (2), 511−517.

(38) Laporte, S.; Magistrato, A. Deciphering the Molecular Terms of Arp2/3 Allosteric Regulation from All-Atom Simulations and Dynamical Network Theory. *J. Phys. Chem. Lett.* **2021**, *12* (22), 5384−5389.

(39) Socher, E.; Conrad, M.; Heger, L.; Paulsen, F.; Sticht, H.; Zunke, F.; Arnold, P. Mutations in the B.1.1.7 SARS-CoV-2 Spike Protein Reduce Receptor-Binding Affinity and Induce a Flexible Link to the Fusion Peptide. *Biomedicines* **2021**, *9* (5).525

(40) Wu, N. C.; Yuan, M.; Liu, H.; Lee, C. D.; Zhu, X.; Bangaru, S.; Torres, J. L.; Caniels, T. G.; Brouwer, P. J. M.; van Gils, M. J.; Sanders, R. W.; Ward, A. B.; Wilson, I. A. An Alternative Binding Mode of IGHV3−53 Antibodies to the SARS-CoV-2 Receptor Binding Domain. *Cell Rep.* **2020**, *33* (3), 108274.

(41) Barnes, C. O.; Jette, C. A.; Abernathy, M. E.; Dam, K. A.; Esswein, S. R.; Gristick, H. B.; Malyutin, A. G.; Sharaf, N. G.; Huey-Tubman, K. E.; Lee, Y. E.; Robbiani, D. F.; Nussenzweig, M. C.; West, A. P., Jr.; Bjorkman, P. J. SARS-CoV-2 neutralizing antibody structures inform therapeutic strategies. *Nature* **2020**, *588* (7839), 682−687.

(42) Ju, B.; Zhang, Q.; Ge, J.; Wang, R.; Sun, J.; Ge, X.; Yu, J.; Shan, S.; Zhou, B.; Song, S.; Tang, X.; Yu, J.; Lan, J.; Yuan, J.; Wang, H.; Zhao, J.; Zhang, S.; Wang, Y.; Shi, X.; Liu, L.; Zhao, J.; Wang, X.; Zhang, Z.; Zhang, L. Human neutralizing antibodies elicited by SARS-CoV-2 infection. *Nature* **2020**, *584* (7819), 115−119.

(43) Wu, Y.; Wang, F.; Shen, C.; Peng, W.; Li, D.; Zhao, C.; Li, Z.; Li, S.; Bi, Y.; Yang, Y.; Gong, Y.; Xiao, H.; Fan, Z.; Tan, S.; Wu, G.; Tan, W.; Lu, X.; Fan, C.; Wang, Q.; Liu, Y.; Zhang, C.; Qi, J.; Gao, G. F.; Gao, F.; Liu, L. A noncompeting pair of human neutralizing antibodies block COVID-19 virus binding to its receptor ACE2. *Science* **2020**, *368* (6496), 1274−1278.

(44) Barnes, C. O.; West, A. P., Jr.; Huey-Tubman, K. E.; Hoffmann, M. A. G.; Sharaf, N. G.; Hoffman, P. R.; Koranda, N.; Gristick, H. B.; Gaebler, C.; Muecksch, F.; Lorenzi, J. C. C.; Finkin, S.; Hagglof, T.; Hurley, A.; Millard, K. G.; Weisblum, Y.; Schmidt, F.; Hatziioannou, T.; Bieniasz, P. D.; Caskey, M.; Robbiani, D. F.; Nussenzweig, M. C.; Bjorkman, P. J. Structures of Human Antibodies Bound to SARS-CoV-2 Spike Reveal Common Epitopes and Recurrent Features of Antibodies. *Cell* **2020**, *182* (4), 828−842.

(45) Liu, L.; Wang, P.; Nair, M. S.; Yu, J.; Rapp, M.; Wang, Q.; Luo, Y.; Chan, J. F.; Sahi, V.; Figueroa, A.; Guo, X. V.; Cerutti, G.; Bimela, J.; Gorman, J.; Zhou, T.; Chen, Z.; Yuen, K. Y.; Kwong, P. D.; Sodroski, J. G.; Yin, M. T.; Sheng, Z.; Huang, Y.; Shapiro, L.; Ho, D. D. Potent neutralizing antibodies against multiple epitopes on SARS-CoV-2 spike. *Nature* **2020**, *584* (7821), 450−456.